

Metamagnetism and Weak Ferromagnetism in Nickel (II) oxalate crystals

E Romero-Tela¹, M E Mendoza¹ and R Escudero²

¹Instituto de Física, Benemérita Universidad Autónoma de Puebla, Apartado Postal J-48, Puebla 72570, México

²Instituto de Investigaciones en Materiales, Universidad Nacional Autónoma de México, Apartado Postal 70-360, México DF 04510, México

E-mail: evarotel@gmail.com

Abstract. Microcrystals of orthorhombic nickel (II) oxalate dihydrate were synthesized through a precipitation reaction of aqueous solutions of nickel chloride and oxalic acid. Magnetic susceptibility exhibits a sharp peak at 3.3 K and a broad rounded maximum near 43 K. We associated the lower maximum with a metamagnetic transition that occurs when the magnetic field is about ≥ 3.5 T. The maximum at 43 K is the typical of 1D antiferromagnets, whereas weak ferromagnetism behavior was observed in the range of 3.3 to 43 K.

PACS numbers: 75.10.Pq; 75.30.Et; 75.50.Xx

Submitted to: *J. Phys.: Condens. Matter*

1. Introduction

It has been shown, theoretically and experimentally, that if a critical magnetic field H is applied along the crystalline anisotropy axis of an antiferromagnet (AF), there occurs a nearly 90° rotation of the sublattice vectors. An antiferromagnetic material with such a behavior is known as a metamagnet [1, 2]. This behavior has been observed in compounds like: $CuCl_2 \cdot 2H_2O$ [3], $FePt_3$, YCO , $TiBe_2$ [4], and $Ni(C_2O_4)(bpy)$, where $bpy = 4,4'$ -bipyridine ($C_{10}H_8N_2$) [5], when applying high magnetic fields (from 10 to 50 T). The type of ordering in $Fe(C_2O_4)(bpy)$, and $Co(C_2O_4)(bpy)$ is also antiferromagnetic but with canted spins. This uncompensated antiferromagnetism produces weak ferromagnetism (WF). Recently, investigations in the quasi-one-dimensional magnetic compound $\beta - CoC_2O_4 \cdot 2H_2O$ [6] revealed that the intra and interchain magnetic interactions tilt the spins, distorting the antiferromagnetic order and producing the WF.

The orthorhombic β -phase of nickel oxalate dihydrate belongs to the space group $Cccm$ with cell parameters $a = 11.842(2)$ Å, $b = 5.345(1)$ Å, and $c = 15.716(2)$ Å [7]. In this structure, oxalate bridges link Ni^{2+} ions chains along the b direction [8, 9, 10, 11] and they mediate a dominant antiferromagnetic intrachain superexchange interaction [12]. Its molar susceptibility data exhibits the broad rounded maximum typical of 1D antiferromagnets with $T_{max} \sim 41$ K [13].

In this paper we report results on the synthesis, crystal structure, and magnetic measurements of the orthorhombic $\beta - NiC_2O_4 \cdot 2H_2O$ microcrystals. We determined by isothermal $M - H$ measurements, from 2 to 80 K, that this phase exhibits weak ferromagnetism in the range of 3.3 to 43 K. At low temperature a metamagnetic order is observed under an applied field ≥ 3.5 T, in $\chi - T$ measurements.

2. Experimental Methods

The synthesis of β - nickel oxalate dihydrate under nitrogen atmosphere was carried out by precipitation reaction of aqueous solutions of nickel (II), chloride 0.1 M (Aesar, 99.9995 %) and oxalic acid 0.00625 M (Baker, ≥ 99.9 %), following the chemical equation,



The precipitates were filtered and dried at room temperature. Morphological analyses were performed with a scanning electron microscope (SEM) Cambrige-Leica Stereoscan 440. Powder X-ray diffraction patterns were acquired using a Siemens D5000 diffractometer operating in the Bragg-Brentano geometry with $\lambda(Cu-K\alpha) = 1.541$ Å, and 2θ scan from $10 - 70^\circ$, and step size of 0.02° . Thermogravimetric (TG) and differential thermal analysis (DTA) curves were obtained in a SDT-TA Instruments model 2960 in air atmosphere with a heating rate of 5 °C/min, from room temperature up to 600 °C. Magnetization measurements were done with a Quantum Design MPMS SQUID

magnetometer, MPMS-5. Zero Field Cooling (ZFC) and Field Cooling (FC) cycles were performed at magnetic field intensities from 0.01 T to 5.00 T, in the range 2 up to 250 K. Isothermal magnetization measurements $M(H)$ were obtained from 2 K - 80 K. The diamagnetic contribution calculated from Pascal's constants [14] was $\chi_{Di} = -72 \cdot 10^{-6} \text{ cm}^3/\text{mol}$.

3. Results and Discussion

3.1. Synthesis

Prismatic green microcrystals of nickel oxalate dihydrate were obtained after eight days of growth in nitrogen atmosphere. Figure 1 presents a SEM micrograph of the crystals with average length size (L) and diameter (D) of 1.47 and 0.65 μm , respectively. Chemical analysis by digestion/ICP-OEP, combustion/TCD/IR-detection and Pyrolysis/IR-detection, gave the composition in weight of 31.82 % in nickel, 13.21 % in carbon, 2.48 % in hydrogen and 51.00 % in oxygen.

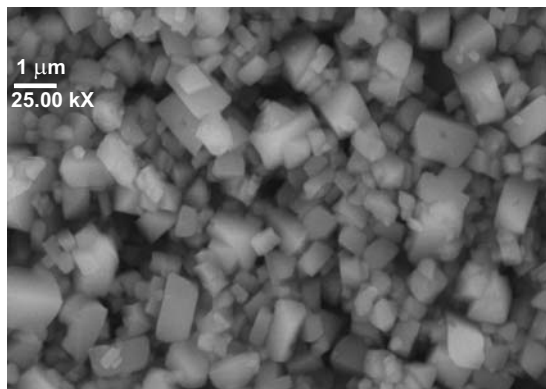


Figure 1. SEM micrographs of β nickel oxalate dihydrate shows prismatic-like shapes. Average length size (L) and diameter (D) were 1.47 and 0.65 μm , respectively.

3.2. Structural characterization

Figure 2a displays the XRD powder diffraction pattern of $\text{NiC}_2\text{O}_4 \cdot 2\text{H}_2\text{O}$ (blue pattern); it is in good agreement with the reported (red lines) for the orthorhombic β -phase of cobalt oxalate dihydrate (JCPDS file: 25-0250). This figure also shows the Rietveld profile fit (red pattern). In figure 2b the difference pattern (red) obtained by using the Win-Rietveld software [15]. Background was estimated by linear interpolation and the peak shape was modeled by Pseudo-Voigt function. Unit cell parameters were $a = 11.842 \text{ \AA}$, $b = 5.345 \text{ \AA}$, and $c = 15.716 \text{ \AA}$ [7]. The atomic positions were the reported by Deyrieux et al., for iron-oxalate [10]; i.e. $4\text{Co}(\frac{1}{4}, \frac{1}{4}, 0)$, $4\text{Co}(0, 0, \frac{1}{4})$, $8\text{C}_{oxalate}(\frac{1}{4}, \frac{1}{4}, 0.042)$, $8\text{C}_{oxalate}(0, \frac{1}{2}, 0.042)$, $16\text{O}_{oxalate}(\frac{1}{4}, 0.0941, 0.089)$, $16\text{O}_{oxalate}(0, 0.691, 0.339)$, $8\text{O}_{water}(0.423, \frac{1}{4}, 0)$, and $8\text{O}_{water}(0.173, 0, \frac{1}{4})$. The weighted

profile and expected residuals factors obtained in the refinement were $R_{wp} = 32.52$, and $R_{exp} = 13.52$.

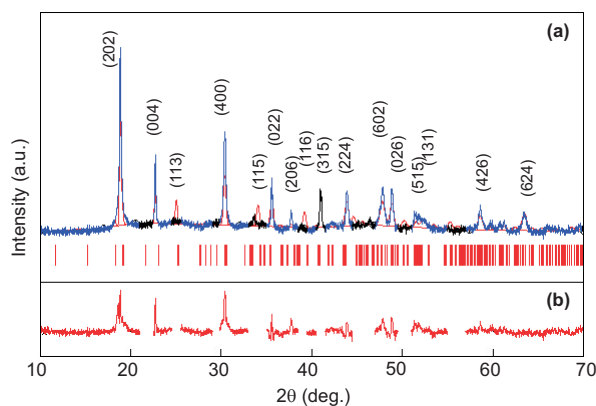


Figure 2. (Color online) (a) X-ray powder diffraction pattern of nickel oxalate dihydrated (blue), peaks absent (black), Rietveld calculated pattern (red) and Miller index (red lines) reported for the orthorhombic $Cccm$ phase (JCPDS file: 25 - 0250). (b) Difference pattern (red).

It must be noticed that some low intensity calculated peaks were absent in the experimental pattern (black peaks in Fig. 2a), this could be due to the method of preparation.

Refined cell parameters determined for the orthorhombic phase of Ni-oxalate sample were $a = 11.759(3) \text{ \AA}$, $b = 5.327(1) \text{ \AA}$, and $c = 15.654(4) \text{ \AA}$. Schematic representation of the unit cell is shown in Fig. 3. There are two non equivalent positions for nickel ions, designed as Ni1 and Ni2, each nickel ion is shifted one respect to of other by a translation vector $(\frac{1}{2}, \frac{1}{2}, 0)$.

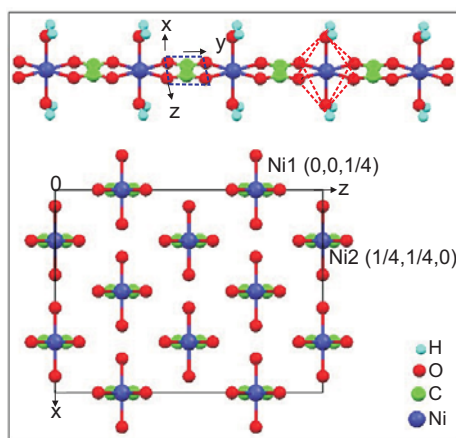


Figure 3. (Color online) Ni-oxalate unit cell of the orthorhombic β -phase of JCPDS file 25-0250, space group $Cccm$. The eight nickel atoms are located in two non-equivalent positions designed as Ni1 and Ni2.

Finally, the coherent diffraction size (D) for the sample crystallites was calculated with the Scherrer equation [16] using the (202) peak, the calculated value was 21.4 nm.

3.3. Thermal analysis

Figure 4 shows the TG and DTA curves of $NiC_2O_4 \cdot 2H_2O$. Two steps of weight loss were observed. The first one ending at 188 °C and the second one finishing at 318 °C. In the first step the weight loss of 19.93 % corresponds to the loss of two water molecules, which agrees with the theoretical value of 19.73 %. DTA curve associated with this process shows an endothermic peak at 188 °C. The dehydration reaction is:



The weight loss about 36.23 % in the second step may be associated to the decomposition to the anhydrous nickel oxalate to nickel oxide, this agrees with the theoretical value of 39.85 % [17, 18]. The corresponding DTA curve shows an exothermic peak, at $T = 318$ °C. The decomposition reaction in this step can be written as

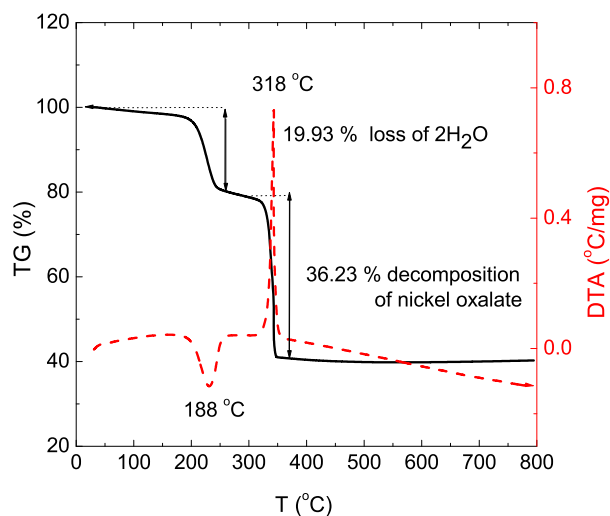
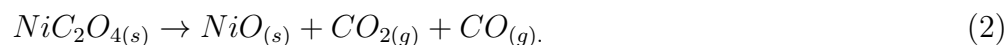


Figure 4. (Color online) The TG (solid line) / DTA (dash line) curves for $NiC_2O_4 \cdot 2H_2O$ at 5 °C/min heating rate.

3.4. Magnetic measurements

The molar susceptibility $\chi(T)$, for the sample is shown in Fig. 5. It was measured by applying magnetic fields of 0.01 T, 0.50 T, and 5.00 T in both ZFC, and FC modes. The main panel shows two well defined maxima in the susceptibility at 3.3 K and 43 K.

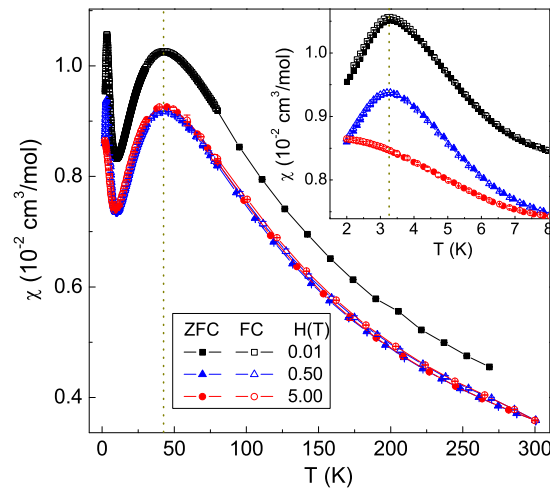


Figure 5. (Color online) Main panel: molar susceptibility of $\beta - NiC_2O_4 \cdot 2H_2O$ with maximum at around 43 K, for both ZFC and FC modes, measured with three applied fields: 0.01 T, 0.50 T and 5.00 T. Inset: displays the susceptibility at low temperature. The maximum at about 3.3 K changes and disappears when the applied magnetic field exceeds 5 T.

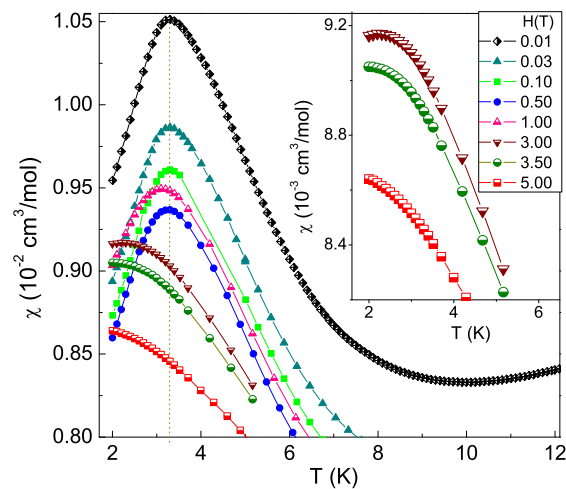


Figure 6. (Color online) This figure presents in the main panel the Molar susceptibility at low temperature with applied fields from 0.01 to 5.00 T, clearly is seen the evolution of the molar susceptibility with increasing field. The Inset displays three curves measured with magnetic fields from 3 to 5 T. At a field about 3.5 T the maximum at 3.3 K disappears.

We also observed changes in the susceptibility at 3.3 K when the magnetic field exceeds 5 T, as mentioned in the caption of figure 5.

Figure 6 shows susceptibility measurements $\chi(T)$, at magnetic fields from 0.01 T to 5 T. Those results indicated that at a field of 3.5 T, the peak at $T = 3.3$ K disappears. This change in the magnetic behavior is related with a metamagnetic transition. Thus, the applied field ≥ 3.5 T, in this compound, is the critical field at which the constraints of crystal field are exceeded, and the magnetic behavior changes.

These results can be compared with those found in other Ni^{2+} systems. Evidences of a metamagnetic transition in $Ni(C_2O_4)(bpy)$ was also obtained in polycrystalline materials [5]. The transition has been anticipated by slope changes in $M(H)$ with higher applied fields, i.e., $H > 30$ kG and below $T_N = 26$ K. In this compound, the one-dimensional magnetic character can be enhanced by replacing the transaxial aquo group by organic groups, such as bipyridine. This has the effect of reducing the interchains interaction and consequently the Néel temperature, and the critical fields required for the metamagnetic transitions [19, 20]. Important examples about these behavior are $CoCl_2 \cdot 2H_2O$, and $\alpha - Co(pyridine)_2Cl_2$ [21]. The details of the magnetic properties of these materials are best understood by examining single crystal data because the transitions are sensitive to the orientation of the applied field [1].

It is important to mention that in Fig. 5, we show that the magnetic susceptibility presents a wide maximum at about 43 K. From 100 K to room temperature $\chi(T)$ smoothly decreases, and a paramagnetic Curie-Weiss behavior can be fitted. The maximum value at 43 K changes with the magnetic field applied as shown in this figure. The changes are on the range from 0.91×10^{-2} to $1.03 \times 10^{-2} \text{ cm}^3/\text{mol}$. This behavior is quite similar to the reported in other compounds, as $Ni(pip)(C_2O_4)$, where pip= piperazine, which is formed by chains of $[Ni(ox)]_n$ and $[Ni(pip)]_n$. In that example, a broad maximum is observed and occurs at 53(1) K [22]. So, accordingly the broad maximum in the susceptibility in our compound is a typical behavior of a low dimensional antiferromagnetic system [23].

In Fig. 7 we show a plot of the inverse of susceptibility, $\chi(T)^{-1}$ at $H = 0.01, 0.50$ and 5.00 T, for $\beta - Ni_2O_4 \cdot 2H_2O$. The analysis of these measurements was performed by fitting a Curie-Weiss from room temperature to 100 K. The fit parameters were Weiss temperature θ_w and Curie constant C varying from -76.90 to -99.82 K and from 1.35 to $1.67 \text{ cm}^3\text{mol}^{-1}\text{K}$, respectively.

The fit parameters could be used to calculate the effective magnetic moment μ_{eff} per mole from equation $\mu_{eff} = 2.84[C]^{1/2} = 2.84 [\chi T]^{1/2}$, which is shown in figure 8.

An important aspect of the behavior μ_{eff} , for this compound, and related to Curie constant, and the large negative Weiss constant, is indicative of a significant antiferromagnetic exchange interactions between neighbouring nickel ions, and a big degree of frustration [24]. It is quite possible because the metamagnetic transition obtained in figures 5 and 6. As observed, this dramatic change of the μ_{eff} is the effect of the change of the Curie constant, and then via the number of unpaired electrons. Thus, accordingly to $\mu_{eff} = g[n(n+1)]^{1/2}$, the number of unpaired electrons n in $NiC_2O_4 \cdot 2H_2O$

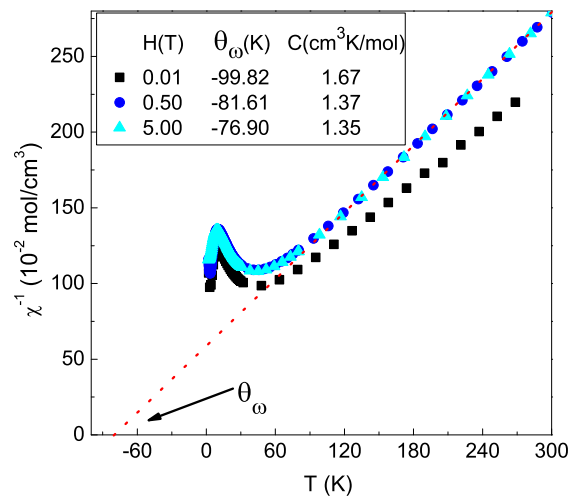


Figure 7. (Color online) Inverse susceptibility at different magnetic fields, $\chi^{-1}(T)$ for dihydrate nickel oxalate. The Weiss temperature θ_ω , changes from about -76.90 to -99.82 K. The Curie constant also changes from 1.35 to 1.67 cm³mol⁻¹K, from high to low magnetic fields.

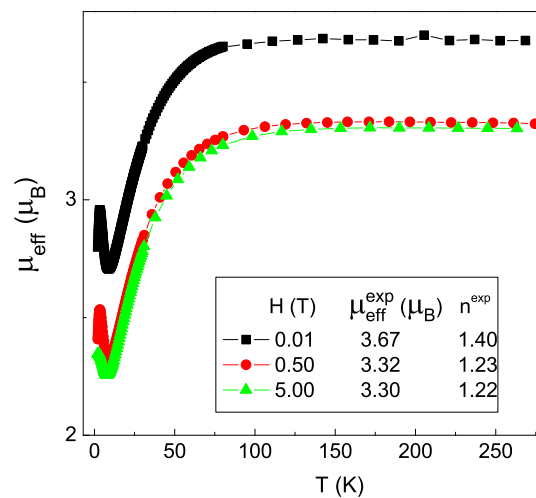


Figure 8. (Color online) Effective Bohr magneton moments μ_{eff} per mol as a function of temperature. At room temperature the values change from 3.30 to about 3.67 μ_B , depending on the magnetic field applied. n^{exp} is the number of unpaired electrons.

can be calculated as 1.40, 1.23 and 1.22 respectively for applied field of 0.01 T, 0.50 T and 5.0 T.

In order to understand more about the magnetic characteristics of this oxalate, we studied the $M - H$ isothermal measurements from the temperature range 2 - 80 K (see figure 9), from these data we extracted the coercive field, which shows a small measurable and perceptible exchange bias. Our measurements of the coercive field, although small, were carefully checked and are below of the possible errors. The results are displayed in figure 10.

This exchange bias can be explained as the effect of inter and intra chains interactions in this compound. The interaction of metallic ions between chains is at the origin of spin canting. This small but measurable exchange bias indicates that instead of produce a pure antiferromagnetic order, the magnetic order has been distorted by canted spins giving rise to weak ferromagnetism. Since weak ferromagnets are a delicate balance of opposing forces, it is not surprising to find that many are also metamagnets [25].

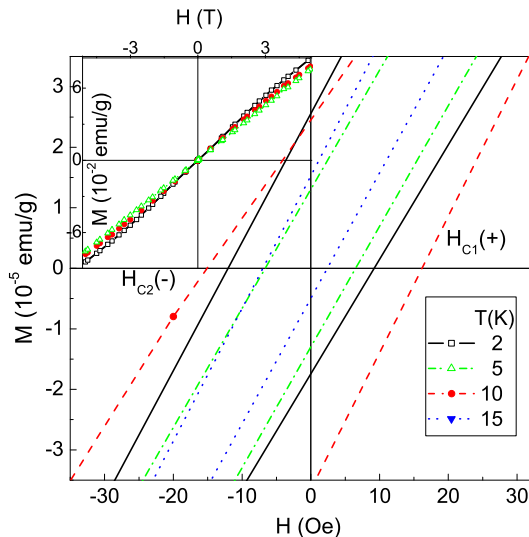


Figure 9. (Color online) Isothermal magnetization measurements $M - H$ from 2 to 15 K shown in the main panel. Note the coercive field and the small exchange bias. Inset shows the $M(H)$ measurements at 4 T and different temperatures from 2 to 80 K. At low fields (main panel) the hysteric effect is clearly observed. The asymmetric behavior in the coercive field is related to a exchange bias effect due to canted spins, but other type of interaction is not discarded as driven by Dzyalochinsky-Moriya type exchange (DM).

Experimentally, it is important to mention that great care was taken when measuring the exchange bias. Our SQUID magnetometer is provided with a Mu metal shielding. At the moment of performing the magnetization measurements a flux gate magnetometer was used to demagnetize the superconducting coil. This procedure

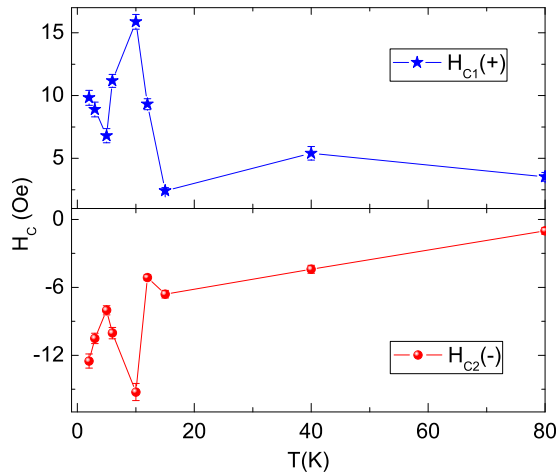


Figure 10. (Color online) Coercive Field vs Temperature determined by isothermal magnetic measurements.

reduces the magnetic field to a very small value to about 0.001 G or less and the μ shielding eliminates external magnetic influences, as the earth magnetic field.

4. Conclusions

Microcrystals single phase of orthorhombic nickel (II) oxalate dihydrate were prepared by soft solution chemistry, as observed by XRD powder diffraction. Chemical analysis, DTA and TG studies revealed that the microcrystals are of high purity. $\chi(T)$ measurements showed the existence of two maxima at 3.3 K and at 43 K. The first one at low temperature changes and disappears with applied magnetic field, this change is due to metamagnetic transition, the maximum disappears with applied field about ≥ 3.5 T. The second maximum indicates an antiferromagnetic order, with interactions due to coupled chains via inter- and intrachain interactions and/or DM type-exchange. The effects of interchain interactions disturb the AF coupling, distorting it and canting spins, which in turn produces a weak ferromagnetic order. This WF is evident by hysteresis measurements in M-H isothermal measurements.

Acknowledgments

Partial support for this work is gratefully acknowledge to CONACyT, project No.44296/A-1 and Scholarship CONACyT, register No. 188436 for E. Romero; VIEP-BUAP, project No. MEAM-EXC10-G. RE, thanks to CONACyT Project 129293(Ciencia Básica), DGAPA-UNAM project No. IN100711, project BISNANO 2011, and project PICCO 11-7 by The Department of Distrito Federal, México.

References

- [1] Keffer F and Chow H 1973 *Phys. Rev. Lett.* **31** 1061
- [2] Jones E R Jr And Stone J A 1972 *J. Chem. Phys.* **56** 1343
- [3] Liu T, Zhang Y, Wang Z and Gao S 2006 *Inorg. Chem.* **45** 2782
- [4] Hurd C M 1982 *Contemp. Phys.* **23** (5) 469
- [5] Yuen T, Lin C L and Mihalisin T W 2000 *J. Appl. Phys.* **87** 6001
- [6] Romero E, Mendoza M E and Escudero R 2011 *Phys. Status Solidi B* **248** 1519
- [7] Deyrieux R, Berro C and Pénéloux A 1973 *Bull. Soc. Chim. Fr.* **1** 25
- [8] Dubernat P J and Pezerat H 1974 *J. Appl. Cryst.* **7** 378
- [9] Molinier M, Price D J, Wood P T and Powell A K 1997 *J. Chem. Soc., Dalton Trans.* 4061
- [10] Deyrieux R and Pénéloux A 1969 *Bull. Soc. Chim. Fr.* 2675
- [11] Drouet C, Pierre A and Rousset A 1999 *Solid State Ionics* **123** 25
- [12] Kurmoo M 2009 *Chem. Soc. Rev.* **38** 1353
- [13] Vaidya S, Rastogi P, Agarwal S, Gupta S K, Ahmad T, Antonelli A M, Ramanujachary K V, Lofland S E and Ganguli K 2008 *J. Phys. Chem. C* **112** 12610
- [14] Bain G A and Berry J F 2008 *J. Chem. Educ.* **85** 532
- [15] McCusker L B, Von Dreele R B, Cox D E, Louër D and Scardi P 1999 *J. Appl. Cryst.* **32** 36
- [16] Cullity B D 1978 *Elements of X-Ray Diffraction*, Second edition (Addison-Wesley)
- [17] Zhan D, Cong C, Diakite K, Tao Y and Zhang K 2005 *Thermochim. Acta* **430** 101
- [18] Zakharov A N, Mayorova A F and Perov N S 2008 *J. Therm. Anal. Cal.* **92** 747
- [19] Otieno T and Thompson R C 1995 *Can. J. Chem.* **73** 275
- [20] Mao L, Rettig S J, Thompson R C, Trotter J and Xia S 1996 *Can. J. Chem.* **74** 433
- [21] Foner S, Frankel R B, Reiff W M, Wong H and Long G J 1978 *J. Chem. Phys.* **68** 4781
- [22] Keene T - D, Ogilvie H R, Hursthouse M B, and Price D J 2004 *Eur. J. Inorg. Chem.* 1007
- [23] Bonner J C and Fisher M E 1964 *Phys. Rev.* **135** A640
- [24] Ramirez A P 2001 *Handbook of Magnetic Materials* **13** (Edited by K. H. J. Buschow) 423
- [25] Stryjewski E and Giordano N 1977 *Adv. Phys.* **26** (5) 487